Pharmacological Research 159 (2020) 104986

Contents lists available at ScienceDirect

Pharmacological Research

journal homepage: www.elsevier.com/locate/yphrs

An innovative method for screening and evaluating the degree of diabetic retinopathy and drug treatment based on artificial intelligence algorithms

Qiwei Xie[a,1], Yanfei Liu[b,c,1], Hui Huang[d,1], Bei Hong[e], Jinxin Wang[d], Hua Han[f,g,**], Yue Liu[b,*]

[a] Research Base of Beijing Modern Manufacturing Development, Beijing University of Technology, Beijing, 100124, China
[b] Cardiovascular Disease Centre, Xiyuan Hospital of China Academy of Chinese Medical Sciences, Beijing, 100091, China
[c] Graduate School, Beijing University of Chinese Medicine, Beijing, 100029, China
[d] Beijing Duan-Dian Pharmaceutical Research & Development Co., Ltd., Beijing, China
[e] Research Center for Brain-inspired Intelligence, Institute of Automation, Chinese Academy of Sciences, Beijing, China
[f] National Laboratory of Pattern Recognition, Institute of Automation, Chinese Academy of Sciences, Beijing, China
[g] School of Future Technology, University of Chinese Academy of Sciences, Beijing, China

ARTICLE INFO

Keywords:
Diabetic retinopathy
Artificial intelligence
Method
Hematoxylin-eosin
Chinese medicine

ABSTRACT

Current methods of evaluating the degree of diabetic retinopathy are highly subjective and have no quantitative standard. To objectively evaluate the slight changes in tissue structure during the early stage of retinal diseases, a subjective interpretation and qualitative analysis of the pathological sections of retinal HE in diabetic animals is required for screening and evaluating the degree of diabetic retinopathy and drug efficacy. To develop an innovative method for screening and evaluating the degree of diabetic retinopathy and drug treatment based on artificial intelligence algorithms. Based on the change law of the early nerve fiber layer and the ganglion cells, we get disparate characteristics of the microscopic image of diabetes animal retina HE slices. Using image recognition and deep learning methods on these HE slices, we can identify the changes in the ganglion cells and nerve fiber layer for diagnosing early retinopathy and evaluated the therapeutic effect of the potential drugs. We conduct quantitative calculation per unit length of the nerve fiber layer and total area of the nerve fiber layer to identify biology significance of edema. Additionally, we also perform quantitative calculation with the number of unit area ganglion cells to identify the section in biology cell hyperplasia. Finally, we get the significance of quantitative calculation on the unit cell area to identify ganglion cell shriveling in biology. In addition to the evaluation of the disease degree and changes, we also obtained retinal HE sections after different drug interventions and evaluated the therapeutic effect of the drugs. This study presents a novel quantitative method for screening and evaluating of diabetic retinopathy and drug efficacy.

Significance of This study

What is already known about this subject?

(1) The pathological traits of DR in the early stage are the obstruction of blood vessel endothelial cells and pericyte function.
(2) Drug efficacy is evaluated by observing the pathological changes in the stained rat or mice retina during preclinical drug development.
(3) Methods of evaluation for the degree of retinopathy are highly subjective and have no quantitative standard in diabetic animals.

What are the New Findings?

(1) Define three biological indicators objectively evaluate the slight changes in tissue structure during the early stage of retinal diseases
(2) Design a two-step traditional processing method to identify the nucleus and the boundary of the RNFL.
(3) Present a novel quantitative pipeline based on the deep convolutional neural network to automatically analyze the area of the retinal nerve fiber layer and the nuclear.

How might these results change the focus of research or clinical practice?

(1) Presents a novel quantitative method for screening and evaluating

* Corresponding author at: Cardiovascular Disease Centre, Xiyuan Hospital of China Academy of Chinese Medical Sciences, Beijing, China
** Co-Corresponding author: National Laboratory of Pattern Recognition, Institute of Automation, Chinese Academy of Sciences, Beijing, China
E-mail addresses: hua.han@ia.ac.cn (H. Han), liuyueheart@hotmail.com (Y. Liu).
[1] Qiwei Xie, Yanfei Liu and Hui Huang contributed equally to this work.

https://doi.org/10.1016/j.phrs.2020.104986
Received 10 March 2020; Received in revised form 5 May 2020; Accepted 29 May 2020
Available online 02 June 2020

of diabetic retinopathy and drug efficacy
(2) It provides a powerful methodological platform for the research and development of new drugs of DR

1. Introduction

Diabetic retinopathy (DR) is a common complication resulting from diabetes mellitus (DM), which represents an indicator or is associated with increased cardiovascular risk and mortality [1,2]. It is a chronic and progressive disease that affects vision and may even result in blindness [3]. The pathological traits of DR in its early stage are the obstruction of blood vessel endothelial cells and pericyte function, causing vascular structural changes, hyperplasia, and leakage. The retinal nerve fiber layer (RNFL) is a bundle of fibers formed by the aggregation of ganglion cell axons, and it tends to be thin, which thickens as diabetes progresses. This change often precedes or is accompanied by vascular leakage and regeneration [4,5]. This is coupled with ganglion cell hyperplasia and cell nucleus edema or shrinkage. The increase in the number of cells and decrease in the area of individual cells can be observed under a microscope. Therefore, the pathological changes associated with diabetic retinopathy in the nerve fiber layer can be assessed by measuring the RNFL area, the number of ganglion cells, the cell area, and other parameters.

During the preclinical drug development, drug efficacy is often evaluated by observing the pathological changes in the stained rat or mice retina. However, current methods of evaluation are highly subjective and have no quantitative standard. The existing methods give a visual description of the lesions, and minor changes within the groups may be undetectable to the human eyes. Additionally, it is difficult for the human eye to perceive changes in the retina, which has a multilayer structure. It is difficult for the human eyes to judge the alteration in the thickness of the nerve fiber layer, changes in the number and the morphology of nuclei in the layer. To aid human perception, image recognition and deep learning have been widely used in the field of biomedicine and retinal image analysis [6]. The method described in this study applied image recognition and deep learning algorithms to analyze retinal Hematoxylin-eosin (HE) sections, which used innovative defined parameters and measurements to provide an objective evaluation of the disease state and drug efficacy.

Hence, this method is an innovative and valuable tool in the development of drug treatments for diabetic retinopathy. Calcium dobesilate (Cal) acts on the endothelial cell layer and the basal layer of hair cell blood vessels by regulating and improving capillary permeability and flexibility. It is commonly used in the market for microangiopathy, including diabetic retinopathy. In this study, it was utilized as one of the positive control. Qiming Granule (QM) is a proprietary Chinese medicine containing Astragalus, Radix Pueraria, Radix Rehmanniae, etc., which has been used for the clinical treatment of type 2 diabetic retinopathy [7] for about ten years in China. In this study, it is used as the other positive control for Traditional Chinese Medicine (TCM), which plays an important role in healthcare in Asia. Tang Wang Ming Mu Granule (TWMM) is a Chinese herb that may be a potential diabetic retinopathy treatment [8]. The aim of this study is to establish automatic image recognition and the deep learning method to systematically obtain evidence for the efficacy of effective drugs in treating diabetic retinopathy and provide an applicative value for clinical translation.

2. Materials and methods

2.1. Animals

Specific pathogen-free (SPF) healthy KKAy mice (males, 8 w) and Wistar rats (males, 8 w, 170 g–190 g) were purchased from Beijing Huafukang Biotechnology Co. Ltd. (Beijing, China, SCXK (Jing):2017 − 0001). The animals were housed at the experimental animal center of Peking University School of Stomatology with controlled temperature (22 ± 2 °C) and humidity (50 % ± 5%) on a 12 -h alternate light-dark cycle. Food and water were provided ad libitum throughout the experiments. The study was authorized by the Animal Care and Ethics Committee of Xiyuan hospital of China academy of Chinese medical sciences and the processes complied with the China National Institutes of Healthy Guidelines for the Care and Use of Laboratory Animals.

2.2. Materials

The extracts of TWMM were kindly provided by Beijing Red Sun Pharmaceutical Co., Ltd (Cat. No. 20130829). Qi Ming granules were purchased from Zhejing Wan Sheng Pharmaceutical Co., Ltd (Cat. No.141023). Calcium dobesilate capsules were purchased from Beijing JingFeng Pharmaceutical Co., Ltd (Cat. No. 141105).

2.3. Streptozotocin-induced diabetes mellitus in rats

We injected the rats with STZ (50 mg/kg BW, dissolved in sodium citrate buffer, pH 4.4), whereas the rats in the control group were without STZ injection. Type 2 diabetic rats were fed with high-fat diet for 5 weeks before STZ injection and continued to be fed with the identical diet until the end of the experiment. We used nondiabetic rats as controls (Group I) and randomized diabetic rats into six groups (Group II ~ VII). Group I and Group II (diabetic controls) received an equal volume of vehicles. Diabetic rats received the antidiabetic retinopathy agent Calcium dobesilate capsules (Cal, 0.15 g/kg BW, i.g) (Group III) or Qi Ming granules (QM, 1.4 g/kg BW, i.g) (Group IV), or TWMM (3.6 g/kg BW, i.g. [Group V] or 7.2 g/kg BW, i.g. [Group VI] or 14.4 g/kg BW, i.g. [Group VII]).

2.4. The experimental protocol

We randomly divided DM animals into six groups (ten animals per group). Using an intragastric tube daily, experimental groups orally ingested TWMM, or Qi Ming granules, or Calcium dobesilate capsules for 8 weeks. We recorded the body weight and fasted blood glucose (FBG) weekly of all rats.

2.5. Histopathologic examination

To prepare harvested tissue sections for the examination by light microscopy, we preserved the retina in the phosphate buffer saline solution with 4% paraformaldehyde, and stained it with hematoxylin and eosin (H & E) for histological evaluation. Pathological pictures of retinas were taken at 400× under an optical microscope (Olympus BX51, Japan). The Retinal injury was evaluated by changes in structure and neovascularization of the retinal internal limiting membrane (ILM).

2.6. Retinal capillary morphology

Retinal digest stretched preparation was used to observe retinal capillary morphology, and to count the numbers of pericytes (PC/mm^2 capillary area) and vascular endothelial cells (EC/mm^2 retinal area), according to published methods (Dietrich and Hammes, 2012).

2.7. Statistical analysis

Statistical analysis was performed with SPSS software, version 11.5 (Armonk, NY, USA). All data were expressed as the mean ± SD. Comparisons between groups were analyzed by one-way ANOVA, and group comparisons were analyzed using the Student-Newman-Kewman-Keuls test. A value of $P < 0.05$ or less was viewed as statistically significant. Sex was not considered a factor in the statistical analysis of the data.

3. Results

3.1. A quantitative analysis and detection platform for the early diabetic retinopathy HE section

According to the experience of the pilot study, we take the animal eye retina HE staining slice in above 12 weeks for preparation, and acquire 20 trials of the retinal image under the microscope, and satisfy the condition that each section of HE has at least five full view fields. Retinal HE sections of Spontaneous type 2 diabetic KKAy mice of different week-old were taken in the same way to meet the requirements of having at least full view fields per HE section.

According to the results of previous studies [8], the retinal HE sections of 12-week-old type 1 diabetic rats showed hyperplasia of the inner boundary membrane, edema of the nerve fiber layer, and disordered arrangement of some ganglion cells. The features of retinopathy in type 2 diabetic rats and spontaneous type 2 diabetic KK mice were different from those in type 1 diabetic rats, showing thinning of the nerve fiber layer and the increasing number of ganglion cells. It has also been reported that ultrastructural changes like ganglion cells occurred in diabetic rats within one month of onset [9].Therefore, based on the early pathological features of DR, such as RNFL thickness, the cell number and cell shrinkage, we artificially defined the area of the nerve fiber layer as total S (S_e), the length of the nerve fiber layer as L, the number of nuclei in the nerve fiber layer as A, and the total area of nuclei in the nerve fiber layer as S_A (Fig. 1 A).

S_e/L was defined as EI, which was considered as the thickness of the nerve fiber layer. When there is nerve fiber layer edema, the total area of the layer increases. In order to eliminate the difference in the size of the selected field of vision under the microscope, we divide the total area by the circumference of the layer, and the EI obtained can reflect the edema degree of the RNFL. A/S_e was taken as the number of unit nuclei, that is, the number of unit nuclei was defined as hyperplasia index HI. As the number of cells increases, the HI value grows. S_A/A is deemed as the unit nuclear area and defined as shrinkage index SI, reflecting the average area size of each cell. SI increases when there is cell edema, and decreases when there is cell shrinkage.

Because the nerve fiber layer in the HE section was very thin under 20 x microscopes and the cell number was scattered randomly, we matched the corresponding image recognition method in line with the actual sample size. According to the amount of the data set, we design two pipelines for automatically quantifying the area of the RNFL and the nucleus, including the deep convolutional neural network (CNN), traditional pattern recognition and image processing (Fig. 1 B,C). Specifically, if the sample size is larger than 100 effective retinal slices, the RNFL and the nucleus of the rat retina were automatically quantified by training a deep neural network. Otherwise, an adaptive threshold method is integrated with the curve fitting model to identify the RNFL's nuclei and boundaries. Therefore, based on the above characteristics of changes in the nerve fiber layer and ganglia cells during the lesion period of DR and the significance of quantitative parameters defined accordingly, we can use these three biological indicators (EI, SI and HI) to quantitatively evaluate the lesion degree in the early stage of DR (Fig. 1 **D**).

3.2. An automatic quantitative measurement platform for the nerve fiber layer and ganglion cells

In the light of the good results of deep learning in natural scene images and biological image [6,10,11], we proposed a fully convolution

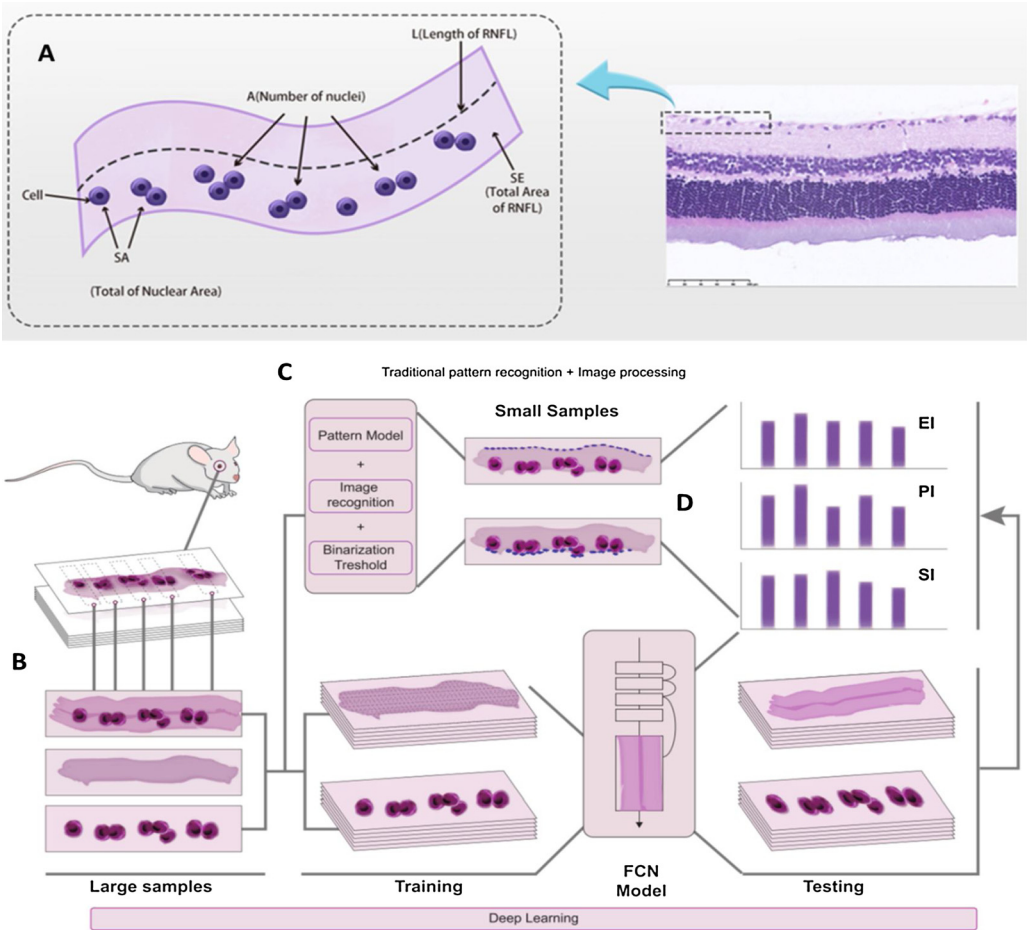

Fig. 1. The Overview of the Data and the Proposed Framework.
The parameter defined in the nerve fiber layer of the retinal HE section, B. automatic quantification frameworks of the RNFL and nuclei by training deep neural networks for HE pathological slice data of the rat retina, C. an adaptive threshold method and a novelty curve fitting model proposed for automatic quantification of nuclei and the RNFL for small batches of data using traditional pattern recognition and image processing, D. the retained nuclei by fusing the results of the RNFL and nuclei, and the area of the total nuclei determined from the area of all connected domains.

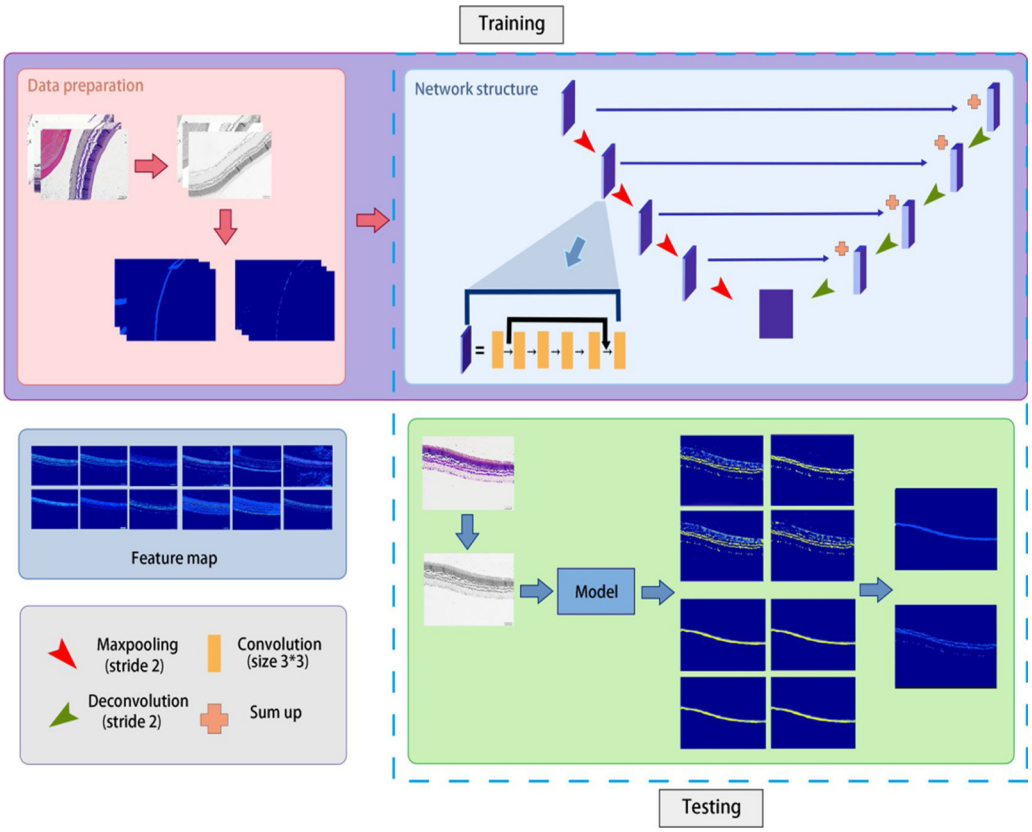

Fig. 2. The Identification Pipeline for Deep Learning.
Data preparation: we converted the RGB image into the grayscale image, and normalized the intensity of the pixel. Network structure: consisting of a downsampling subnetwork, an upsampling subnetwork, and skip connections between blocks of the same level and different paths. Model training: we fed the data and label into the network architecture to learn the hyperparameters. Model testing: through the trained decision hyperparameters, we inferred the unknown test data and segment the specific structure.

network framework to automatically segment the RNFL and nuclei. In our problem, there are overlapping regions between the RNFL and the nucleus, thus limiting the use of multi-category segmentation networks, which will lead to ambiguity. To effectively perform segmentation for overlapping regions, we employed two binary segmentation networks to predict the probability maps of the RNFL and the nucleus in the image. The pipeline consists of the following five parts as shown in Fig. 2 (see **supplementary file** for details).

3.3. Image recognition results of the nerve fiber layer based on small samples

Deep learning provides efficient recognition ability. However, it also requires a lot of data and significant effort to annotate the data. [12]. Consequently, in scenarios where we have limited training data, we propose to apply the traditional processing method which did not require too much prior information. As shown in Fig. 2, we introduced a novel analysis flow in this section, which adopted an adaptive threshold and designed a curve fitting model successively to identify the nucleus and the boundary of the RNFL. When the sample size was less than 100 effective slices, we used the two-step method, that is, the upper boundary of the nerve fiber layer was obtained using the traditional image processing method. On this basis, an effective fitting model of the boundary was designed (see **supplementary file** for details).

3.4. Image recognition results of ganglion cells in the layer of nerve fibers

The number of the nucleus was often a key factor in pathological analysis. Accurate quantization of the number of nuclei in HE slices was perceived as a challenging task, mainly because some nuclei were clustered. We handled this challenge by means of the number of connected domain pixels, the median of the number of connected domain pixels and watershed transformation, respectively (see **supplementary file** for details).

3.5. Quantitative accuracy analysis results

To assess the effectiveness of the two proposed methods, we measured the several segmentation metrics of the two methods in the test dataset separately. For the RNFL, the results showed that the average precision and recall of AI technology are 94.63 % and 87.09 %, respectively, while the corresponding traditional methods are 90.36 % and 83.62 %, and both F1 and the Jaccard index could achieve above 0.7 For the nucleus, the F1 score and Jaccard of the two methods are 77.08 %, 62.78 and 71.90 %, 56.78 % respectively, which indicated the performance of deep learning was better than the traditional method. For the statistics result of the number of nuclei, our method could be close to the result of the human count, and the relative deviation generated by the watershed transformation was similar to or even slightly lower than that of the manual counting (0.1136 and 0.1218, respectively), indicating the stability and effectiveness of our methods (see **supplementary file** for details).

3.6. Assessment of disease progression using deep learning

In order to verify the above automatic analysis algorithm, we specially selected retinal HE sections of KK mice aged 18 W, 22 W, 26 W, 30 W, 34 W and 38 W and C57 mice at corresponding time points, and five sections were randomly selected for each experimental group. By employing the above deep learning method, EI, SI and HI were calculated and statistical in Fig. 3

The results showed that, compared with normal C57 mice, the EI of KK mice did not alter significantly in 18 w, 22 w, 26 w and 30 w, suggesting that there was no prominent edema in the retinal nerve fiber layer. Nevertheless, at 34 w and 38 w, EI was significantly reduced and the neural fiber layer was distinctly thinner (Fig. 3A), which was also consistent with the rule of retinopathy in type 2 diabetic mice, that was, the tendency of thinning appeared first and then progressed in the stage of thickening the neural fiber layer. At the same time, KK mice showed

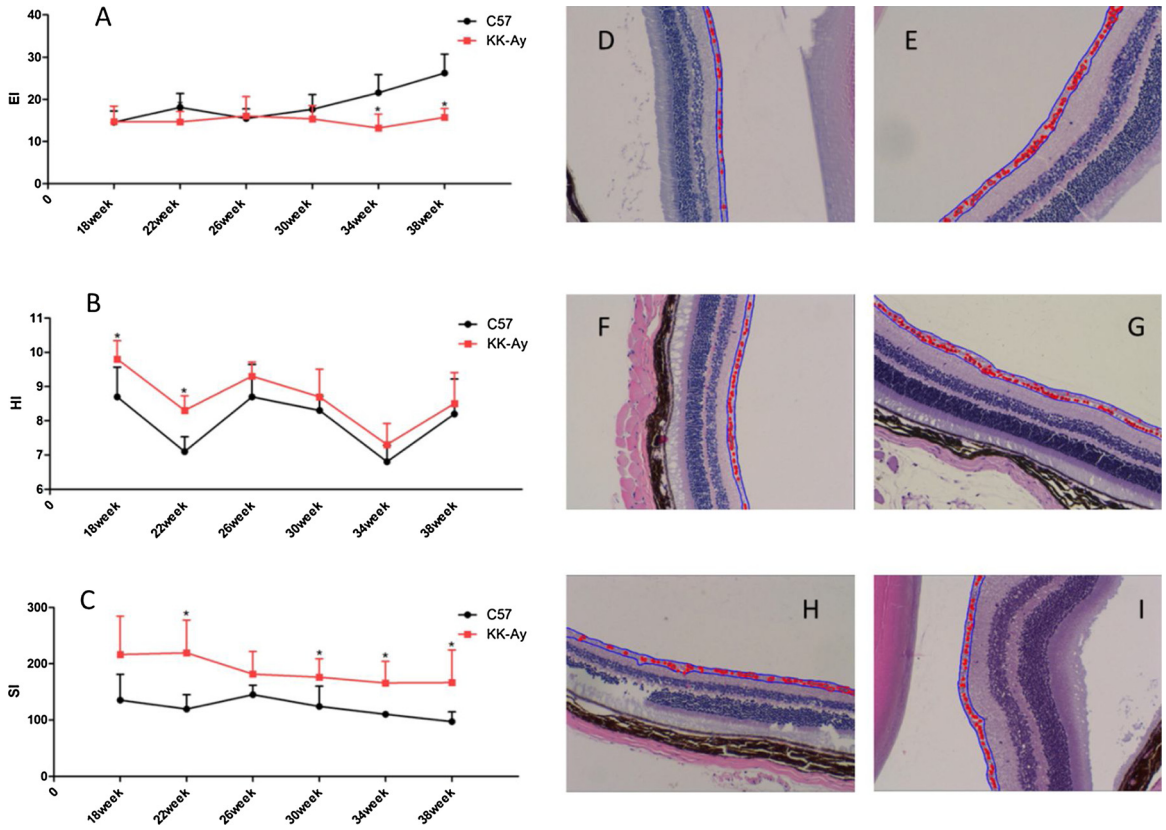

Fig. 3. Results of quantitative analysis of retinal HE images in KKAy mice and C57 mice.
A. changes of the retinal nerve fiber layer edema index in KK mice and C57 mice at different time points, B. changes of the nuclear hyperplasia index of the retinal nerve fiber layer in KK mice and C57 mice at different time points, C. changes of the nuclear shrinkage index in KK mice and C57 mice at different time points, D. HE image (magnified 20 x) of 18 W KKAy, E. HE image of 22 W KKAy, F. HE image of 26 W KKAy, G. HE image of 30 W KKAy, H. HE image of 34 W KKAy, and I. HE image of 38 w KKAy. *Significant differences ($P < 0.05$) between model group and corresponding control group.

a substantial increase in HI in 18 W and 22 w (Fig. 3B), indicating that the ganglion cells of the KK mice showed an evident proliferation phenomenon. In the subsequent time points, it could be seen that the HI of the KK mice increased compared with that of the normal mice, but no statistical difference was found (Fig. 3C), which might be suggested that a much more accurate method of efficacy evaluation was provided. KK mouse SI was significantly increased at each time point, and there was a statistical difference between sections of KK mice in 22 w, 30 w, 34 w and 38 w and the normal group, signifying that there was an obvious swelling of ganglion cells. HE slices from the same sample have been read by pathologists. When reading the report, due to the naked eye observation, a pathologist could not accurately judge if the number of the nucleus changes and was not sensitive for early extremely slight pathological changes. It also reflected that the image recognition method based on the deep learning had the very ideal sensitivity compared with the naked eye observation.

3.7. Drug efficacy assessment

From various experiments, we selected 611 regions with uniform target regions, including the nerve fiber layer region and the ganglion cell region. The deep learning (340 regions) and the pattern recognition method (271 regions) mentioned above were used to establish the corresponding algorithm, the STZ-induced type 1 diabetes rat model and the model of STZ-induced type 2 diabetes rats with high-fat feeding. Biological samples of each drug administration group were collected together, and the RNFL edema, nuclear shrinkage or edema, and cell hyperplasia were quantitatively assessed in accordance with the above customized parameters.

The results showed that, compared with biological indicators in the normal group, EI was significantly increased in the model group of type 1 diabetes (Fig. 4 A1); HI was significantly decreased and was statistically significant (Fig. 4 A2); SI showed a trend of decrease but no statistical difference (Fig. 4 A3). Nevertheless, type 2 diabetic rats presented a significant decrease in EI and an increase in HI (Fig. 4 B1/B2), which was in keeping with the pathological features of KK mice with spontaneous type 2 diabetes. High fasting blood glucose was the initial factor of diabetic microvascular lesions, and the degree of retinal and renal lesions in type 1 diabetes was more serious than that in type 2 diabetes [13]. From our results, we also found that the retinal neurofibrillary lesion in type 2 diabetic rats was in the thinning stage, while that in type 1 diabetic rats had developed to a more severe thickening stage. There was no significant change in SI for either type 1 or type 2 diabetic rats (Fig. 4 B3), indicating that no significant swelling or shrinkage of lower ganglion cells was observed in the two models, which differed from that in KK mice and may be related to the characteristics of disparate animal models. Also, we will calculate and analyze 271 HE sliced microscopic images of type 2 diabetic rats with the above traditional processing method. Various parameter results are found to be consistent with the large sample study results of the deep learning (Fig. 4 C1/C2/C3), and the standard deviation of the results of traditional pattern recognition is greater than that of deep learning results reflecting the difference between the two methods as well.

The results demonstrated that Calcium dobesilate capsules, Qiming granules and different doses of TWMM could significantly reduce the EI value of type 1 diabetic rats, indicating that the symptoms of edema of the nerve fiber layer were relieved (Fig. 4 A1). HI in type 1 diabetic rats was significantly lower than that in the normal group (Fig. 4 A2), mainly due to disordered arrangement of ganglion cells. However, different drug interventions could make the arrangement of ganglion

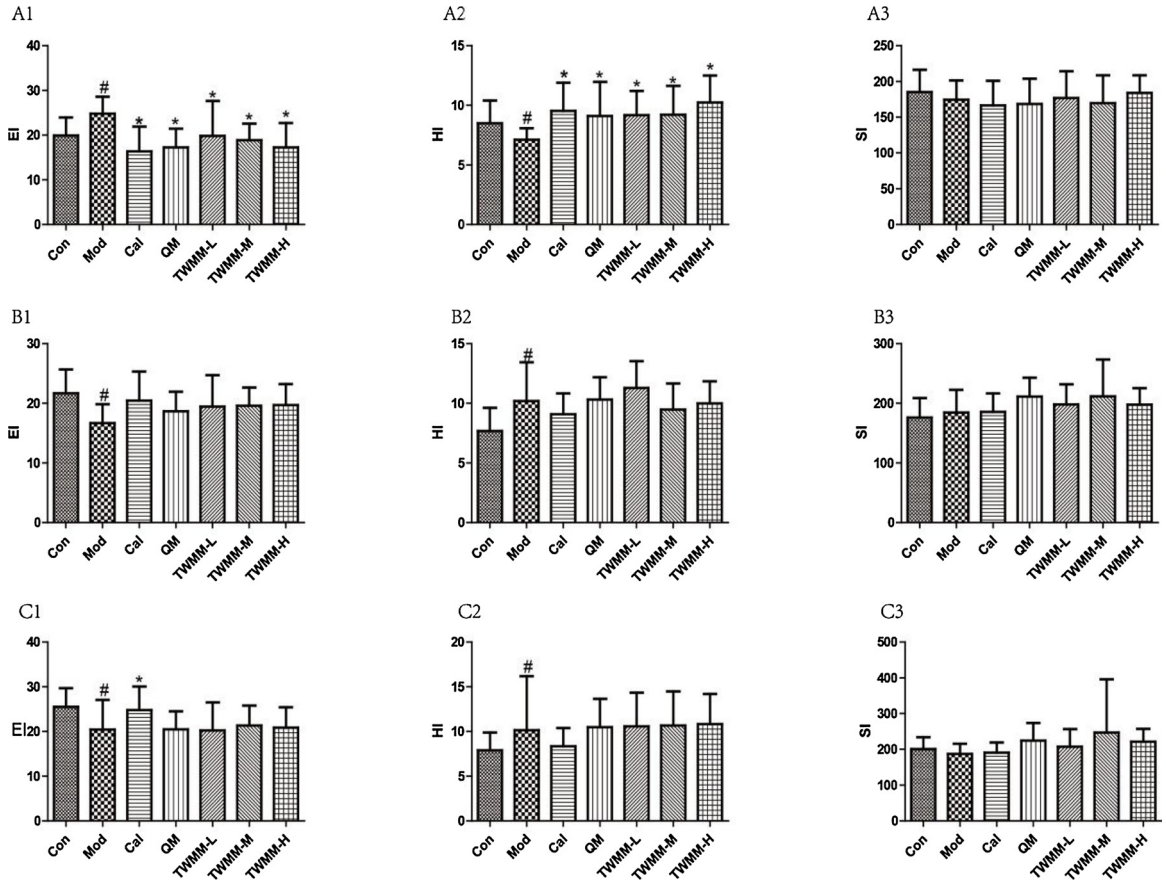

Fig. 4. Deep learning and pattern model methods used to evaluate the degree of disease and efficacy of drugs in type 1 and type 2 diabetic rats.
A1 − 3. parameters of the deep learning method of the type 1 diabetes animal model, B1 − 3. parameters of the deep learning method of the type 2 diabetes animal model, and C1 − 3. parameters of the pattern recognition method of the type 2 diabetes animal model. #$P < 0.05$, compared with the corresponding control group ; *$P < 0.05$, compared with the corresponding model group.

cells more regular, and the number of cells identified by deep learning results showed an increasing trend, which was also in line with the literature report [8]. After drug intervention in type 2 diabetes rat models, the trend of improving EI and HI was observed, but there was no statistical difference compared with the model group (Fig. 4), which might be suggested that a much more accurate method of drug efficacy evaluation was provided in this paper compared with the previous approach.

The results of Fig. 4 were further verified by biological experiments. The pathological examination was made on HE sections and transmission electron microscopy(TEM) images from the same biological sample first. The conclusion drawn by the pathologist for HE sections was that the retinal layers in the normal control group had complete structure, the regular arrangement and normal cell morphology. Hyperplasia or loose edema appeared in the inner boundary of the membrane of the model group. The TWMM group had different degrees of improvement on the inner boundary membrane structure and cell morphology, inhibiting neovascularization. The same effect could also be observed in the QM and Cal groups. The observed results of TEM showed that the structure of retinal capillaries was intact; peripheral cells and endothelial cells were normal; organelles and nuclei were normal. In the model group, some basal membranes of capillaries were thickened and pleats in the cytoplasmic membrane were apparent. Edema reduction and visible nuclear morphology were observed in QM group, Cal group and TWMM group with different doses (Fig. 5). Neither HE section nor the transmission electron microscope can make a quantitative evaluation of the lesion degree. As cell shrinkage can simply be observed under the electron microscope, this pathological change was relatively slight. However, we believed that deep learning results can identify even subtle changes after increasing the training sample size.

Changes in the vascular endothelial growth factor (VEGF) and Evans Blue (EB) were investigated. It was noted that the levels of those two parameters were in the same direction (Fig. 6). The DM rats exhibited greatly higher VEGF and EB levels in retinal tissue than those in the normal control rats ($P < 0.05$ and $P < 0.05$, respectively). After 8-week treatment, TWMM markedly reduced VEGF and EB levels in diabetic rats (DM + L-TWMM, DM + M-TWMM, DM + H-TWMM, and $P < 0.05$ vs. DM group). Qi Ming granule treatments also showed significantly reduced VEGF and EB levels ($P < 0.05$ and $P < 0.05$, respectively), and Calcium dobesilate capsule treatments showed the same results ($P < 0.05$ and $P < 0.05$, respectively). These results will show that different drugs have different effect on the treatment of type 2 diabetic rat retinopathy, but reflecting the obvious change in the organizational structure also needs a certain amount of sample size. From the results of the proposed AI method, the trend of drug action can be observed.

4. Discussion

DR is characterized by aberrations in the number and the function of vascular endothelial cells and pericytes, typically manifested as vascular structural alterations, hyperplasia, and leakage. Clinically, DR can be classified into non-proliferative and proliferative stages. The RNFL comprises ganglion cell axons formed along the inner retinal surface toward the optic nerve, and the functional changes of the RNFL are closely associated with the dysfunction of the optic nerve and the vascular endothelium. The RNFL is the most significant and the earliest site of manifestation in retinopathy. For instance, RNFL thinning is a typical initial change during the pathogenesis of DR (*4*), and the

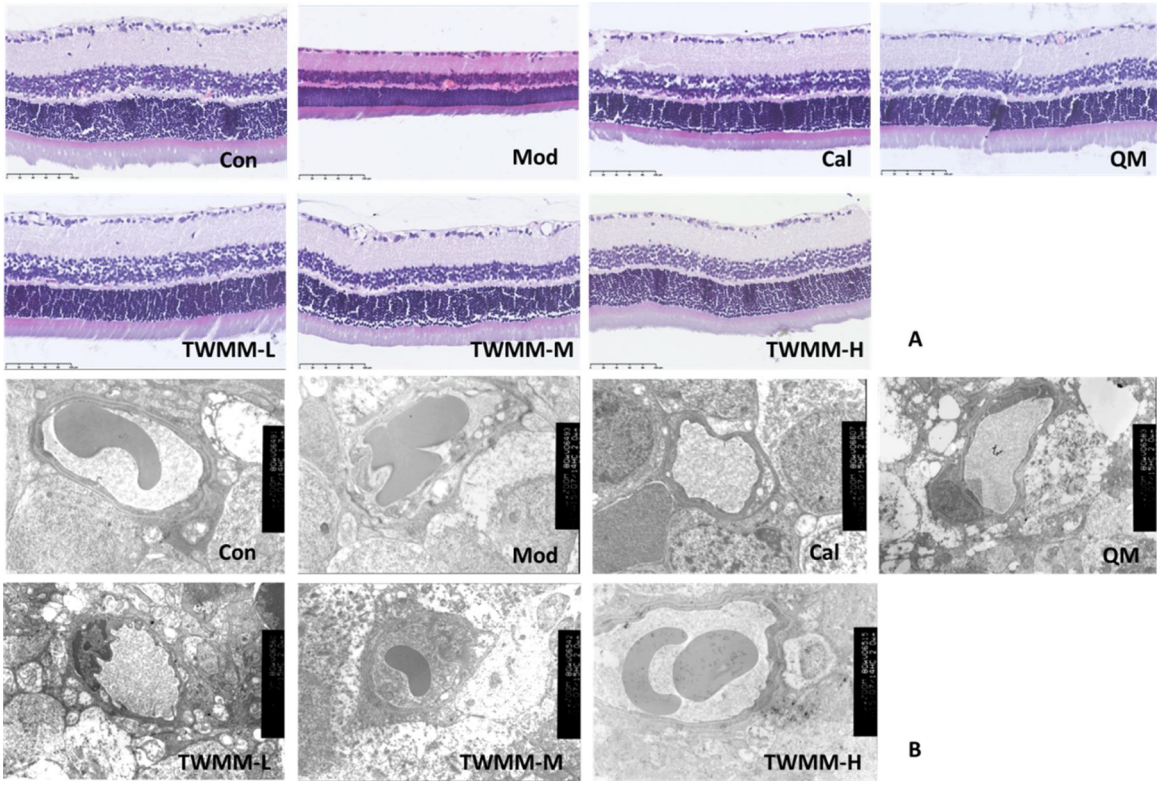

Fig. 5. HE and TEM images of biological samples from type 2 diabetic rats.
A. microscopic images of different groups of HE sections, B. electron microscope images of different groups.

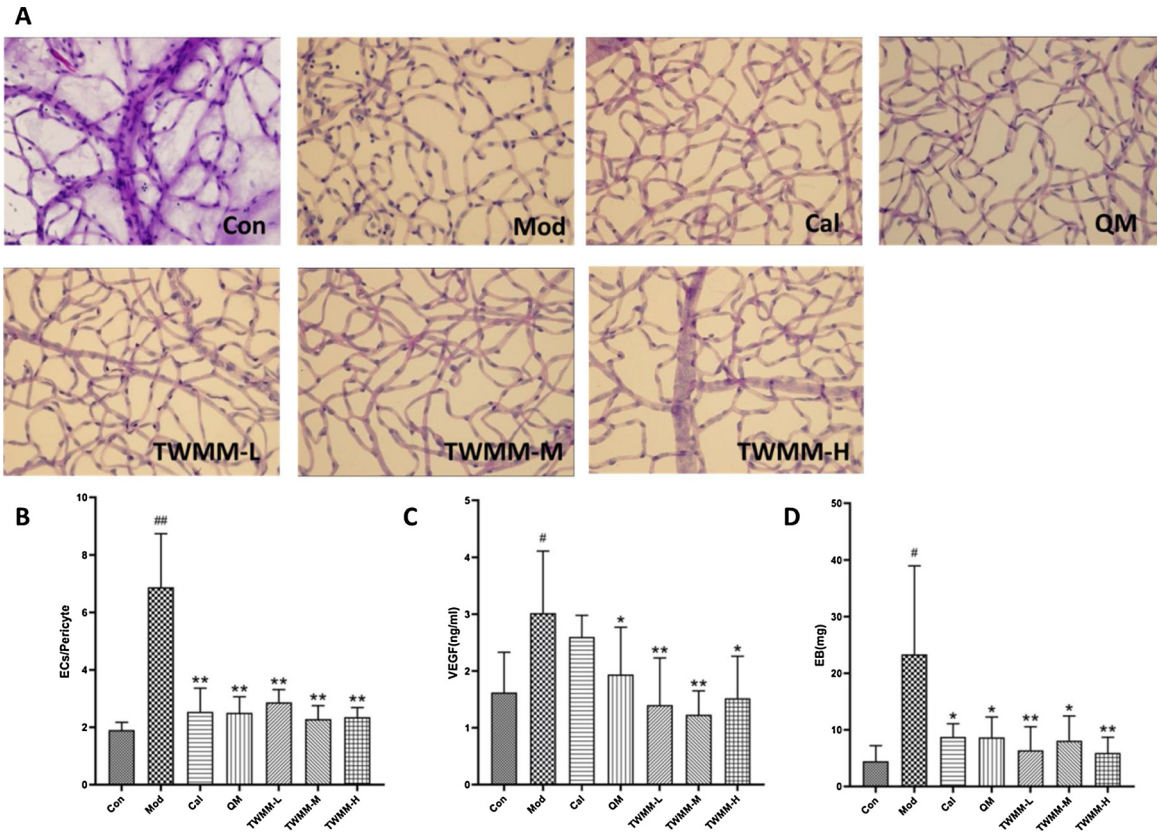

Fig. 6. Changes in the ratio of endothelial cells to peripheral cells and biological indicators in type 2 diabetic rats and drug administration groups.
A. The picture of periretinal cells and endothelial cells of different groups in type 2 diabetic rats. B. The ratio of endothelial and pericyte Numbers. C. VEGF level in blood of type 2 diabetic rats. D. Results of determination of EB content. $\#P < 0.05$, $\#\#P < 0.01$ compared with the corresponding control group ; $*P < 0.05$, $**P < 0.01$ compared with the corresponding model group.

thickness of the RNFL reflects the severity of DR. In addition, changes in RNFL thickness may precede microvascular changes (*5*).

Regarding the importance of the RNFL in the pathogenesis of DR, RNFL thickness has already been introduced as a clinical parameter to assess disease progression in patients. Common methods for measuring RNFL thickness include Scanning Laser Polarimeter (GDx) (*14*), optical coherence tomography (OCT), and fundus photography. However, due to the characteristic spherical structure of the eyeball, the RNFL at different regions of the retina exhibits different thicknesses (in other words, the nerve fiber bundles in the peripapillary vascular network are the thickest). In addition, the border of the RNFL represents an arcuate pattern with different thicknesses in various sections. Comparatively, the measurement of the RNFL area is more objective than measuring its thickness. Therefore, we have artificially defined the total RNFL area as the edema index and utilized it as one of the indicators to assess the severity of early DR lesions. This approach requires automated identification and segmentation of the RNFL layer in the images. Currently, the use of artificial intelligence in pathology is most commonly employed to distinguish and calculate large-scale cancerous and non-cancerous areas in the field of oncology. The most frequently-used methods are the supervised classification andsegmentation of the target areas, and application of corrections to enhance robustness [4]. Some research groups have used the Spectralis software (Heidelberg Engineering) to perform automated RNFL thickness segmentation, but in cases of poor segmentation, manual corrections are required [15]. Furthermore, different retinal layers are closely packed, and the RNFL is thinner than other layers. We had previously tried performing automated RNFL identification using image analysis software, but did not succeed. There have also been attempts to use the multispectral imaging technique to measure RNFL thickness via collecting images of HE stained sections from separate spectral bands. However, this approach has merely achieved simple calculations for the inner nuclear layer that has a flat border [16]. Comparatively, the first-of-its-kind method reported in the present study, which is based on image identification from a small dataset and deep learning from a large dataset, allows for automatic segmentation and calculation of the RNFL border, thereby achieving the quantitative evaluation of early DR lesions.

The RNFL is bound up with the blood-retinal barrier and the volume of the capillary network changes with the thickness of the nerve fiber layer. Hence, a change in the RNFL area indirectly reflects the capillary function. In patients with DR, RNFL thinning is accompanied by damage to the intercellular tight junctions and integrity of the barrier function, which increases vascular permeability [17]. The evidence-based results in type 2 diabetic animals also show that RNFL changes are accompanied by concurrent damage to the blood-retinal barrier, in which the permeability is increased. We have also observed similar phenomena in animal models of type 1 diabetes [8]. Moreover, the RNFL area is relevant to the function of the vascular endothelium, and the vascular endothelial dysfunction is closely connected with the severity of DR and retinal neurodegeneration [18]. Insufficient blood supply can give rise to functional impairment of the optic nerve [19,20]. We also observed from our experiments in different types of diabetic animal models that, while the RNFL areas decreased, levels of the vascular endothelial growth factor (VEGF) in the serum increased. The results from retinal flat mounts also showed noticeable alterations in the number of vascular endothelial cells and pericytes.

Apart from the vascular function, RNFL thickness is associated with many biological indicators, such as serum levels of uric acid [21] and blood lipid levels [5]. Some research groups have attempted to use RNFL images as a useful adjunct for the clinical evaluation of patients with neurological eye disorders [14]. Others have considered RNFL thinning as the primary feature of neovascular glaucoma (NVG) [15], believing that changes in the RNFL preceded other characteristic lesions in glaucoma. Therefore, the RNFL is of vital significance in the study of disease progression and pathogenesis. Furthermore, it has enormous utility in the field of new drug development. Several groups have evaluated the effects of drugs on RNFL loss in diabetic patients by assessing changes in RNFL thickness following drug intervention [5]. Certain drugs can prevent RNFL loss via the modulation of the endothelial dysfunction; this includes the improvement of blood flow, reduction of vascular permeability, the increase in blood supply, and avoidance of neuronal cell death [22]. TWMM granule used in this study can be utilized for the treatment of early DR by improving the vascular endothelial function and reducing vascular permeability. These mechanisms are consistent with the findings of other studies [14].

In addition to changes in RNFL areas, DR also manifests as neurodegenerative changes during the early stages prior to the appearance of vascular abnormalities, with different sorts of nerve cells in different retinal layers exhibiting aberrations and apoptosis [23,24]. Numerous research groups were able to use transmission electron microscopy to observe vacuolar degeneration limited to a small portion of the mitochondria in the cytoplasm of ganglion cells in diabetic animals 1 month after disease onset [6]. This indicates that in addition to the changes in the RNFL, the number and morphological changes of cells are also crucial during the very early stage of DR. Therefore, we have defined 2 additional indices—the nuclear shrinkage index and the hyperplasia index—for the quantitative measurements of the degrees of changes in tissue structures and cells in each sample. During this process, the acquisition of 2 parameters, namely the number of nuclei and the total cell area, is crucial.

The retinal layers are extremely dense, with irregular distribution of nuclei and indiscernible boundaries. In consequence, it is extremely challenging to perform automatic identification, segmentation, and calculation of the cells. Existing software applications similar to InForm (Perkin Elmer) perform automated segmentation for large areas [25]. The automated segmentation for different types of cell nuclei in designated area is difficult to achieve, and the counting results display considerable differences from the actual number. In this study, we made an attempt to perform automated calculation for the number of ganglion cells in the nerve fiber layer and the sum of cell areas, and achieved satisfactory results. Through three algorithms for estimating the number of nuclei, we compared the deviations from the real number, respectively. The stability and accuracy of the statistical method based on the watershed transform even exceeded the manual statistical results.

With the two algorithms proposed in this paper, we could clearly conclude that KK mice, which have inherent glucose intolerance and insulin resistance, exhibited prominent nuclear edema and hyperplasia as disease duration increased. However, a definite conclusion of cell proliferation can be obtained in the model of type 2 diabetic rats induced by STZ and fed with high-fat diet. These conclusions coincide with the results of HE sections and TEM [21], indicating the accuracy and extremely high sensitivity of this method to micropathological changes. This method of automatic cell identification and calculation can also be employed for the classification and calculation of endothelial cells and pericytes in retinal flat mount images.

The fluorescein angiography (OCT) technique, commonly used in clinical settings, can be used to observe microangioma and retinal microvascular morphology and movement, and determine whether the choroid shows pathological changes. It is apparent that this technique focuses on changes in vascular morphology and hemodynamics, and the changes can merely be clearly observed using OCT when DR has developed to a moderate, severe, or proliferative stage [26]. It has been reported that STZ rats fed with a high-fat diet only developed neovascularization at 110 weeks of age than Wistar albino rats [27]. Similarly, these minor changes in the RNFL and cells in the early stage of DR are difficult to be identified accurately using conventional HE-stained sections with the naked eye. Even if the characteristics of the lesions can be detected, the degree of severity of the lesions cannot be quantified. The HE sections in this study were manually reviewed by pathologists. Certain changes in the thickness of the nerve fiber layer

were recorded but other minor cellular changes were not disclosed by the pathologists. Therefore, it is evident that the pathological changes in early DR display high inter-observer variability. In comparison, the definitions of parameters and the acquisition method proposed in the present study can provide advanced guidance for early disease detection, treatment, and drug efficacy evaluation, particularly for the disease stage in which significant vascular changes have not occurred. In this study, we employed this method to analyze the HE sections of retinas from animals after intervention from the drug TWMM and found that compared with the control model group, it can reduce the edema of the nerve fiber layer in type 1 diabetic rats, make the arrangement of ganglion cells more orderly, and reduce the tendency of ganglion cell proliferation in type 2 diabetic rats. These findings showed that retinopathy was relieved, and the conclusion was in accord with that in other publications [8]. In the meanwhile, when the proposed methods were used to validate the efficacy of the QM and Cal drugs currently marketed for the treatment of DR, the results were consistent with their clinical efficacy [28].

The present method is advanced, and its accuracy is significantly superior to the results obtained from manual interpretations, which greatly reduces the work required for manual interpretations of the sections. Compared with hyperspectral or multispectral fundus imaging techniques [25], the present technique overcomes the limitations of the differences in material composition corresponding to different parts of the retina. It does not require the separation of spectral bands from different fundus structures, nor does it require knowledge of the features and differences of structural elements in different layers. All parameters can be easily acquired through automated image identification and machine learning, reducing the requirement of engineering knowledge for the biologists and medical personnel. Moreover, the present method has features of versatility and low technical variability. There are no mandatory requirements for the normalization of the quality and intensity of staining of the tissue specimens, and there is no need to perform full digital scanning on the sections. Images with a certain number of pixels captured by a regular camera will meet the analytical requirements. Meanwhile, this method is highly extensible and can be applied to the analysis of HE section images with similar properties.

Contribution statement

Qiwei Xie, Yanfei Liu and Hui Huang put on the experimental study, data analysis and writing of the manuscript together, are the co-first authors. Yue Liu and Hua Han contributed to the topic conception, manuscript revision, and the decision to submit for publication, are the co-corresponding authors. Bei Hong and Jinxin Wang contributed to data analysis, help to revision of manuscript.

Declaration of Competing Interest

The authors declare that there is no conflict of interest associated with this manuscript.

Acknowledgements

This research is supported by Special Project for Outstanding Young Talents of China Academy of Chinese Medical Sciences (ZZ13-YQ-001), Beijing NOVA Program (No. Z171100001117027). National Natural Science Foundation of China (No. 61673381), Special Program of Beijing Municipal Science & Technology Commission (Z181100003818001,Z181100000118002). the Strategic Priority Research Program, CAS (No. XDB32030200), Bureau of International Cooperation, CAS (No. 153D31KYSB20170059).

Appendix A. Supplementary data

Supplementary material related to this article can be found, in the online version, at doi:https://doi.org/10.1016/j.phrs.2020.104986.

References

[1] D. Pongrac Barlovic, et al., The association of severe diabetic retinopathy with cardiovascular outcomes in long-standing type 1 diabetes: a longitudinal follow-up, Diabetes Care 41 (2018) 2487–2494.
[2] J. Xie, et al., Association of diabetic macular edema and proliferative diabetic retinopathy with cardiovascular disease: a systematic review and meta-analysis, JAMA Ophthalmol. 135 (2017) 586–593.
[3] J.A. Beckman, M.A. Creager, Vascular complications of diabetes, Circ. Res. 118 (2016) 1771–1785.
[4] H. Takahashi, et al., Diabetes-associated retinal nerve fiber damage evaluated with scanning laser polarimetry, Am. J. Ophthalmol. 142 (2006) 88–94.
[5] R. Shi, et al., The effect of fenofibrate on early retinal nerve fiber layer loss in type 2 diabetic patients: a case-control study, BMC Ophthalmol. 18 (2018) 100.
[6] G. Campanella, et al., Clinical-grade computational pathology using weakly supervised deep learning on whole slide images, Nat. Med. 25 (2019) 1301–1309.
[7] X.X. Luo, et al., Effect of qiming granule on retinal blood circulation of diabetic retinopathy: a multicenter clinical trial, Chin. J. Integr. Med. 15 (2009) 384–388.
[8] M. Chen, et al., Tang Wang Ming Mu granule attenuates diabetic retinopathy in type 2 diabetes rats, Front. Physiol. 8 (2017) 1065.
[9] J. Kusari, et al., Effect of memantine on neuroretinal function and retinal vascular changes of streptozotocin-induced diabetic rats, Invest. Ophthalmol. Vis. Sci. 48 (2007) 5152–5159.
[10] J. De Fauw, et al., Clinically applicable deep learning for diagnosis and referral in retinal disease, Nat. Med. 24 (2018) 1342–1350.
[11] S. Dorkenwald, et al., Automated synaptic connectivity inference for volume electron microscopy, Nat. Methods 14 (2017) 435–442.
[12] C. Sun, et al., Revisiting unreasonable effectiveness of data in deep learning era, IEEE International Conference on Computer Vision (2017) 843–852.
[13] S. Park, et al., Recent advances in the pathogenesis of microvascular complications in diabetes, Arch. Pharm. Res. 42 (2019) 252–262.
[14] B.M. Dinkin, et al., Imaging the nerve Fiber layer and optic disc, Essentials in Ophthalmology (2008) 99–118.
[15] S. Yokota, et al., Circumpapillary retinal nerve fiber layer thickness, anterior lamina cribrosa depth, and lamina cribrosa thickness in neovascular glaucoma secondary to proliferative diabetic retinopathy: a cross-sectional study, BMC Ophthalmol. 17 (1) (2017) 57.
[16] Q. Li, et al., Quantitative analysis of protective effect of erythropoietin on diabetic retinal cells using molecular hyperspectral imaging technology, IEEE Trans. Biomed. Eng. 57 (2010) 1699–1706.
[17] S. M. W, Pathophysiology of Diabetic Retinopathy. Diabetic Retinopathy, Springer, New York, NY, 2010, pp. 1–30.
[18] G. Mazereeuw, et al., Platelet activating factors in depression and coronary artery disease: a potential biomarker related to inflammatory mechanisms and neurodegeneration, Neurosci. Biobehav. Rev. 37 (2013) 1611–1621.
[19] J.A. Choi, et al., Retinal nerve fiber layer loss is associated with urinary albumin excretion in patients with type 2 diabetes, Ophthalmology 122 (2015) 976–981.
[20] S. Ozdek, et al., Assessment of nerve fiber layer in diabetic patients with scanning laser polarimetry, Eye Lond. (Lond) 16 (2002) 761–765.
[21] M.N. Vinuthinee-Naidu, et al., Correlation of retinal nerve fibre layer and macular thickness with serum uric acid among type 2 diabetes mellitus, BMC Ophthalmol. 17 (2017) 91.
[22] Y. Hu, et al., Pathogenic role of diabetes-induced PPAR-alpha down-regulation in microvascular dysfunction, Proc Natl Acad Sci U S A 110 (2013) 15401–15406.
[23] A.M. Abu-El-Asrar, et al., Expression of apoptosis markers in the retinas of human subjects with diabetes, Invest. Ophthalmol. Vis. Sci. 45 (2004) 2760–2766.
[24] T.M. Curtis, et al., Muller glial dysfunction during diabetic retinopathy in rats is linked to accumulation of advanced glycation end-products and advanced lipoxidation end-products, Diabetologia 54 (2011) 690–698.
[25] J.T. Handa, et al., Lipoprotein(A) with an intact lysine binding site protects the retina from an age-related macular degeneration phenotype in mice (An american ophthalmological society thesis), Trans. Am. Ophthalmol. Soc. 113 (2015) T5.
[26] V.K. Chanjira Sinthanayothin, et al., Automated screening system for diabetic retinopathy, 3rd International Symposium on Image and Signal Processing and Analysis (2003) 915–920.
[27] J.E. Mancini, et al., Proliferative retinopathy and neovascularization of the anterior segment in female type 2 diabetic rats, Diabetol. Metab. Syndr. 5 (1) (2013) 68.
[28] L. Cheng, et al., Evaluation of hypoglycemic efficacy of tangningtongluo formula, a traditional Chinese Miao medicine, in two rodent animal models, J. Diabetes Res. 2014 (2014) 745419.